Eur Biophys J (2002) 31: 89–101
DOI 10.1007/s00249-001-0196-9

ARTICLE

Indira Chandrasekhar · Wilfred F. van Gunsteren

A comparison of the potential energy parameters of aliphatic alkanes: molecular dynamics simulations of triacylglycerols in the alpha phase

Received: 29 June 2001 / Revised: 31 October 2001 / Accepted: 31 October 2001 / Published online: 8 December 2001

Abstract A comparison of six GROMOS parameter sets for aliphatic alkanes is presented using simulations of a triglyceride, trioctanoin, in the gel or α phase. It is found that the parameter set 43A2 results in a system that is rigid and close packed, forcing a collective tilt of the molecules, known experimentally to be disallowed. The parameter set 45A3-45 results in an expanded system where the molecules undergo a conformational change from the chair to tuning-fork form. The lamellae are fragmented, with the fragments shifted in the direction parallel to the layer normal. The newest parameter set 45A3, when used with either of two sets of partial charges for the glycerol ester group, retains the characteristics of the gel phase. The last parameter set tested, 45A3-45×12, also performs well when combined with either set of partial charges, although the system expands in the plane of the bilayer.

Keywords Molecular dynamics simulation · Lipids · Potential energy parameters

Introduction

The structure and packing characteristics of alkane chains in lamellar membrane systems are known to have profound consequences on their dynamic and thence their phase behaviour, ultimately affecting their physiology (Small 1986; Cevc and Marsh 1987). Clearly, the mechanics and dynamics of these systems are controlled by complex inter-atomic interactions. Molecular dynamics (MD) simulation is the method of choice to evaluate the interactions between molecules at the atomic level and to interpret their effects on the dynamic behaviour of a system. MD simulation has been used fairly extensively on alkane and lipid bilayer systems (Egberts and Berendsen 1988; Tieleman and Berendsen 1996; Merz and Roux 1996; Feller et al. 1997; Husslein et al. 1998; Chiu et al. 1999; Marrink and Mark 2001; Smondyrev and Berkowitz 2000; see also reviews by Pastor 1994; Tieleman et al. 1997; Tobias et al.1997).

Of critical importance to the qualitative and quantitative interpretation of a MD simulation is the force field that calculates the potential energy of the inter-particle interactions and its parameterization. The potential-energy parameters used in simulating biological systems are generally developed by a process of refinement against experimental or ab initio quantum-mechanical data (see, for example, van Gunsteren and Berendsen 1990). The parameterization of classical force fields for lamellar lipid and related systems has proved particularly challenging, demanding frequent refinement (Stouch et al. 1991; Egberts et al. 1994; Schlenkrich et al. 1996; Feller et al. 1997; Chiu et al. 1999; Schuler and van Gunsteren 2000; Schuler et al. 2001). The reasons for this are manifold. Lamellar systems undergo complex polymorphic behaviour. The different polymorphic forms exist within a small temperature and density range and are sensitive to a variety of different variables (Small 1986; Cevc and Marsh 1987). Potential-energy parameters have to be carefully tested in order to reproduce such behaviour with confidence. It has been frequently observed that the particular nature of lamellar lipid systems, which consist of large arrays of similar molecules with medium to long, varyingly flexible alkane chains, results in artefacts during simulation. These artefacts, often related to the potential-energy parameters used, are evident even when the parameters used have proven to be adequate for more dense systems such as proteins or for systems in aqueous solution. For example, early simulations of lipids using united- or extended-atom force fields resulted in an unrealistic tilting of the chains (Bareman and Klein 1990; Chandrasekhar 1992). More recently, the GROMOS96 parameter sets 43A1 (van Gunsteren et al. 1996) and

I. Chandrasekhar (✉) · W.F. van Gunsteren
Laboratory of Physical Chemistry,
Swiss Federal Institute of Technology Zürich,
ETH-Zentrum, 8092 Zurich, Switzerland
E-mail: indira@igc.phys.chem.ethz.ch
Fax: +41-1-6321039

43A2 (Schuler and van Gunsteren 2000) were unable to sustain micelles and bilayers of dipalmitoylphosphatidylcholine (DPPC) in water (Schuler 2000). Many recent simulations of lipid systems make use of all-atom force fields (Feller et al. 1997; Bogusz et al. 2000). However, increasing the number of particles and therefore the number of pair-wise interactions in the system, by the explicit inclusion of hydrogen atoms, can prove expensive. An exhaustive refinement of united-atom parameters to better reproduce liquid alkane properties (Daura et al. 1998; Schuler 2000; Schuler and van Gunsteren 2000; Schuler et al. 2001) has recently been undertaken in our laboratory. The study reveals the interdependence of different parameters and the need for a consistent approach in order to reproduce observable tendencies such as the chain-length dependence of the thermodynamic properties of liquid alkanes. We present an evaluation of six different potential-energy parameter sets developed for the classical MD simulations of lamellar lipid systems. Our simulation system consists of double layers of a simple neutral lipid, the triacylglycerol trioctanoin.

Triacylglycerols, or triglycerides as they are commonly known, are major constituents of natural fats and oils and are indeed the most widely occurring form of lipids stored in plant and animal tissues. Triglycerides undergo complex polymorphism; the multiple melting behaviour of tristearin was observed as early as 1849 (Heintz 1849). The polymorphic forms, melting behaviour and other physical and thermodynamic properties of this class of molecules have been fairly well investigated (Lutton 1950; Malkin 1954; Chapman et al. 1960; Larsson 1963; Callaghan and Jolley 1977; Garti and Sato 1988; Kishore and Shobha 1992; reviews by Larsson 1986; Hagemann 1988; Hernqvist 1988) and a clear picture of the phase behaviour of the molecules has been elucidated. Like the structurally related polar glycerolipids, the neutral triglycerides aggregate in lamellar arrays in the gel and crystalline phases. Fairly detailed conformational and packing information is available from crystallography and molecular modelling studies (Jensen and Mabis 1966; de Jong 1980; van Soest et al. 1990; Birker et al 1991; de Jong et al. 1991; Goto et al. 1992; van Langevelde et al. 2000; Sato et al. 2001), indicating that acyl chain organization varies critically between polymorphic forms. As both short- and long-range forces are believed to affect the behaviour of lamellar systems, it is useful to simulate the intermediate less-ordered phases to examine the efficacy of a given set of potential-energy parameters. We simulate the gel or α phase of trioctanoin.

We see the advantage of using a triglyceride system to evaluate the different potential-energy parameters, as opposed to the more extensively studied model glycerolipids such as DPPC, as follows. Triglycerides are simple molecules consisting of three acyl chains attached to a glycerol group by an ester linkage. Although they are organized in the familiar lamellar arrangements attained by the glycerolipids, they are clearly not amphipathic in nature. Therefore the simulation model contains only triglycerides and no water. This then eliminates various complexities of the polar lipids such as head-group dependence, dependence on degree of hydration, adequate representation of polar solvent, and ionic strength, to name but a few.

In this paper we present constant pressure MD simulations of a 10×10×2 double layer of the gel or α phase of the eight-carbon triglyceride trioctanoin, using different united- or extended-atom parameter sets for non-bonded interactions developed in our laboratory. Six simulations are presented. They make use of the GROMOS96 parameter sets 43A2 (Schuler and van Gunsteren 2000), 45A3 (Schuler et al. 2001) and its variants 45A3-45 and 45A3-45×12 (Schuler 2000), combined with two sets of atom partial charges. To our knowledge, this is the first MD simulation study of triglycerides.

Model and methods

Six simulations, each of a 10×10×2 double-layer array of trioctanoin, were carried out. The simulation models, M1 to M6, differ in the potential-energy parameters sets, which are detailed below.

Potential energy parameters

The semi-empirical potential-energy terms used in classical molecular mechanics and MD calculations have been extensively described (for example, Ramachandran and Sasisekharan 1969; van Gunsteren et al. 1996). We make use of the standard GROMOS96 interaction function (van Gunsteren et al. 1996).

Alkane parameters

During the course of the last few years the potential-energy parameters for aliphatic alkanes have been carefully refined in our laboratory (Daura et al. 1998; Schuler and van Gunsteren 2000; Schuler et al. 2001). The parameters are generally developed by adjusting to the experimental enthalpies of vaporization and liquid densities of a chosen set of alkanes (Daura et al. 1998). As the torsional flexibility of these compounds plays a critical role in their overall organization, the force constants for the dihedral cosine term were fitted to recent experimental and ab initio values for the various barrier heights and relative populations of the different conformers. This process entailed the refitting of the third-neighbour van der Waals parameters, resulting in what is termed the 43A2 parameter set (Schuler and van Gunsteren 2000). Unfortunately, the parameter set 43A2, which is used to carry out the simulations for the model termed M1, did not reproduce micelle and bilayer behaviour in the case of DPPC (Schuler 2000). Therefore the parameter set was further refined by fitting to an extensive range of alkanes, saturated, unsaturated and branched. This led to refined parameters for the aliphatic united atoms, CH_1, CH_2 and CH_3, and to the introduction of two new atom types, type CH_{2r} for CH_2 groups in cyclic structures and type CH_0 for tetrahedral sp^3 carbons bound to four non-hydrogen atoms. This parameter set is called 45A3 (Schuler et al. 2001). Model M2 is based on a variation of the parameter set 45A3: instead of the standard van der Waals parameter for sp^2 carbons in planar groups used in the 43A1, 43A2 and 45A3 parameter sets, the type CH_0 parameters for the tetrahedral sp^3 atom (type number 45) are used to represent the planar ester carbons. This variation on parameter set 45A3 is indicated by 45A3-45 (Schuler et al. 2001). The atom type CH_0 has

a relatively large radius of $\sigma = 0.6639$ nm. The models M3 and M4 make use of the unmodified parameter set 45A3. Models M3 and M4 differ in the partial charges at the glycerol ester group. In the latter case, the ab initio charges for the *sn*-1 chain from the set of charges developed by Chiu et al. (1995) for phosphoglycerolipids are used. In the next pair of simulations (models M5 and M6), yet another value for the van der Waals parameters for the bare planar carbon is used. Here the van der Waals radius is taken to be the geometric mean of that of the bare tetrahedral carbon CH_0 (type number 45) and the united tetrahedral carbon type CH_1 (type number 12) from parameter set 45A3. The consequent parameter set is called 45A3-45×12 (Schuler 2000). Again M5 and M6 differ in the partial charges at the glycerol ester group, with charges from Chiu et al. (1995) replacing the GROMOS96 charges in M6. The different models and parameters are shown in Tables 1 and 2.

Ester group

The bonded interaction parameters for the bonds and bond angles of the ester group have been chosen from the standard GROMOS96 parameters to reproduce the ester geometry, which is not unlike the peptide geometry (see, for example, Chandrasekhar 1986). For the assignment of the torsional parameters at the ester moiety we invoke its similarity to the peptide group. The three relevant torsions are described qualitatively. For clarification of atomic nomenclature, see Fig. 1. The torsion about the bond CG*n*-O*n*1, where *n* refers to the chain number ($n = 1, 2, 3$), assigns the conformation of the first methylene carbon along the alkane chain and has two-fold symmetry. The torsion about the ester bond, O*n*1-C*n*1, has a planar character as may be deduced from its reduced length of 1.33 nm (Table 3). The torsional profile about the bond C*n*1-C*n*2 linking the ester moiety to the alkane chain is fairly flat and the potential energy is dominated by the non-bonded repulsion at the *cis* conformation. The bond, angle and torsional angle parameters are listed in Table 3.

Initial conditions

The molecule in the α phase

We begin by briefly describing relevant aspects of the α phase of triglycerides. As in other polymorphic forms, the molecules in the α phase are believed to be in the "chair" conformation, so named because one of the acyl chains forms the back of a chair and the other two the legs, with the glycerol backbone forming the seat of the chair (Fig. 1). The molecules organize in what is known as the double-layer packing mode, where the molecules stack as shown in Fig. 2 with the "seats of the chairs" adjacent to each other. This is easily ascertained by the fact that here the interlayer spacing is related to two chain lengths rather than three as is seen in some of the more dense crystalline β and β′ forms, where the bilayer packing mode is favoured (Larsson 1986; Hernqvist 1988). Other critical differences between the α form and the β forms are as follows: in the α form (1) the molecules are straight rather than tilted with respect to the layer normal, (2) the chain termini are not interdigitated but rather show evidence of torsional disorder at the interface and (3) the chains pack in a hexagonal sub-cell, although there is some question as to the manner of rotational reorientation (Chapman et al. 1960).

Density and box dimensions

The unit cell dimensions for trioctanoin in the gel phase are unknown. However, given the molecular density per unit cell of similar molecules, the inverse of which yields the unit cell volume, one can make assumptions about the conformation and orientation of the alkane chains to arrive at reasonable starting dimensions.

The density of tristearin in the α phase is 1.014 g cm^{-3} (Bailey and Singleton 1945) and its molecular weight is 891.5 D. Noting that there are two molecules per unit cell in the double-layer packing mode of the α phase (see Fig. 2), the volume per unit cell is 2.919 nm^3. If we make the assumption that the molecule in the fully extended state is oriented along the *z* direction, the length of the unit cell in the *z* direction is equal to the length of tristearin, which is 5.05 nm (for details of the internal geometry, particularly of the ester group, see Table 2). The unit cell area perpendicular to the *z*-axis is then 0.57 nm^2. As there are effectively three extended chains per unit cell (Fig. 2), this implies a cross-sectional area per chain of approximately 0.19 nm^2. Possible choices for the two shorter cell dimensions, in keeping with the pseudo-orthorhombic packing mode of the chains in the hexagonal close-packed system, are 0.43 and 1.34 nm. Here the shorter dimension refers to the axis where the nearest neighbour is one chain apart (in our case *x*) and the longer to the perpendicular direction where the nearest neighbour is three chains away. These dimensions are consistent with hexagonal packing of alkane chains, where the cell dimension per three chains is approximately 1.3 nm (Abrahamsson et al. 1978). The cross-sectional area per chain in our system is 0.192 nm^2. This is at the lower limit for the packing of hydrocarbon chains (Tardieu et al.

Table 1 The van der Waals parameters for the aliphatic alkane carbons of trioctanoin in the united atom representation for each of the parameter sets used. The van der Waals interaction is defined as $4\epsilon[(\sigma/r)^{12}-(\sigma/r)^6]$; ϵ values in kJ mol^{-1} and σ values in nm

Model		CH_3	CH_2	CH_1	Planar C
M1: 43A2[a]	ϵ	0.7323	0.4896	0.3139	0.4059
	σ	0.3875	0.3920	0.3800	0.3361
M2: 45A3-45[b]	ϵ	0.8672	0.4105	0.09489	0.006995
	σ	0.3748	0.4070	0.5019	0.6639
M3/M4:[d] 45A3[c]	ϵ	0.8672	0.4105	0.09489	0.4059
	σ	0.3748	0.4070	0.5019	0.3361
M5/M6:[d] 45A3-45×12[b]	ϵ	0.8672	0.4105	0.09489	0.02577
	σ	0.3748	0.4070	0.5019	0.5773

[a]Schuler and van Gunsteren (2000)
[b]Schuler (2000)
[c]Schuler et al. (2001)
[d]The two models differ in the partial charges of the glycerol ester group, as detailed in Table 2

Table 2 The partial charges (in e) for the glycerol ester groups. The atom numbers are defined in Fig. 1 ($n = 1, 2, 3$)

Model	CG*n*	O*n*1	C*n*1	O*n*2
M1, M2, M3, M5[a]	0.20	–0.36	0.54	–0.38
M4, M6[b]	0.50	–0.70	0.80	–0.60

[a]van Gunsteren et al. (1996)
[b]Chiu et al. (1995). The partial charges from the *sn*-1 chain of the phosphoglycerolipids are used

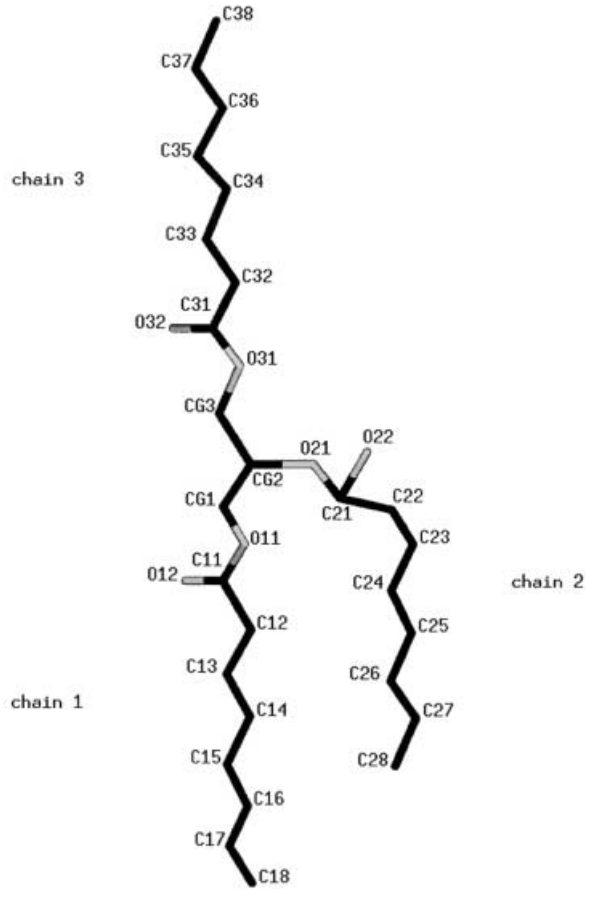

Fig. 1 The triglyceride molecule trioctanoin, in the chair conformation. The atom names are derived from a consistent numbering scheme developed for lipid nomenclature (see Chandrasekhar and Sasisekharan 1989)

1973; Wiener et al. 1989), largely due to the assumption that the chains are fully extended. We expect to see an adjustment of these dimensions in the course of the simulations.

Having determined the approximate dimensions of the unit cell, we construct a computational box consisting of a 10×10 double-layer array for simulation. The GROMOS96 force field is compatible with a long-range cut-off radius of 1.4 nm for the pair-wise interactions (Daura et al. 1998). Using the so-called minimum image convention, the lengths of the computational periodic box must be larger than twice the cut-off radius plus the diameter of a charge group (van Gunsteren et al. 1996). In other words, the box lengths should be greater than 3 nm. The particular juxtaposition of the double-layer packing as opposed to bilayer packing (Fig. 2) implies that the box length in the z direction is approximately equal to the length of one molecule. Even in the fully extended state this is only about 2.53 nm for trioctanoin. We therefore double the system size to include two double layers. In effect, we simulate 400 molecules, each 33 (extended) atoms in size, arranged in two 10×10 double layers of 200 molecules each. The system consists of 13,200 atoms and the initial dimensions of the periodic box are 4.3×13.4×5.05 nm.

Conditions of the simulation

Initial velocities were taken from a Maxwellian distribution at 222 K. Rectangular periodic boundary conditions were applied (details of the box size are discussed above). Initially the system was strongly coupled to a temperature bath of 222 K with a relaxation time of 0.01 ps and to a pressure bath of 1 atm with a relaxation time of 0.05 ps (Berendsen et al. 1984). These simulation conditions were used for 10 ps. Following this, the coupling was switched to the analysis conditions of 0.1 ps for the temperature coupling and 0.5 ps for the pressure coupling (Berendsen et al. 1984). The simulation temperature is 222 K, for which trioctanoin is known to be in the gel or α phase (Hagemann 1988). In all cases, anisotropic pressure coupling was used. The isothermal compressibility, κ_T, for triglycerides was estimated as follows. At room temperature and atmospheric pressure, κ_T for liquid long-chain alkanes such as *n*-octane and *n*-octadecane is of the order 1.66×10^{-3} (kJ mol^{-1} nm^{-3})$^{-1}$ (McGowan 1982). The value for lipids ranges between 0.55 and 1.660×10^{-3} (kJ mol^{-1} nm^{-3})$^{-1}$ (Cevc and Marsh 1987). By comparison, κ_T for water is 0.747×10^{-3} (kJ mol^{-1} nm^{-3})$^{-1}$ and a value commonly used for simulations of proteins in water is 0.45×10^{-3} (kJ mol^{-1} nm^{-3})$^{-1}$ (van Gunsteren et al. 1996). We choose $\kappa_T = 1.0\times10^{-3}$ (kJ mol^{-1} nm^{-3})$^{-1}$ for our simulations. Bond lengths were constrained to ideal values using the SHAKE algorithm (Ryckaert et al. 1977) with a geometric tolerance of 10^{-4}. The time step for the leap-frog integration scheme was set to 2 fs. The non-bonded interactions were treated using a twin-range cut-off scheme (van Gunsteren and Berendsen 1990; Daura et al. 1998). The short-range cut-off radius was 0.8 nm, within which interactions were determined every time step. Long-range interactions were updated every five time steps with a cut-off radius of 1.4 nm. Results are discussed for the equilibrated trajectories, the approach to equilibrium being discussed where relevant.

Results

In the following subsections we discuss the simulation results for each of the models M1 to M6 followed by comments relevant to all the models.

Density and box size

The box dimensions in the x, y and z directions, area per chain, A_c, and the volume of the periodic box for each of the six models are shown in Fig. 3. In all cases the relaxation during the initial heating phase, where the system is coupled to the temperature bath by an order of magnitude tighter than in the simulation run, is not shown.

In the case of model M1, the box dimensions quickly relax during the heating phase, at which stage there is a reduction in the y direction of 1.0 nm. The box dimensions continue to relax until 3.5 ns, when the system reaches equilibrium. Specifically, the x dimension increases while the y dimension decreases, to the plateau values of 4.7 and 12.3 nm, respectively. The box size in the z direction is 4.8 nm at equilibrium and the volume of the system stabilizes at about 280 nm^3. This implies an increase in the density of approximately 4%, relative to the start-up value of 291 nm^3. The average square area per chain, A_c, decreases at first but then regains the start-up value of 0.192 nm^2 at equilibrium (Table 4).

The x and y dimensions of the periodic box in the case of the M2 simulation undergo an initial increase during the heating phase, while the z dimension decreases. At equilibrium the x and y dimensions fluctuate around 5.2 and 13.3 nm, respectively. The box size in the z dimension stabilizes at 4.8 nm and the volume fluctuates about 329 nm^3, the value reached at the end of the

Table 3 Bonded interaction parameters for the ester moiety selected from van Gunsteren et al. (1996), where the functional form of the interaction terms and their parameters have been defined. The atomic nomenclature is given in Fig. 1 (*n* refers to the chain number and is equal to 1, 2, 3)

Bond	${}^{K}b_n$ (10^7 kJ mol^{-1} nm^{-4})	b_n (nm)	
CG*n*-O*n*1	0.871	0.147	
O*n*1-C*n*1	1.18	0.133	
C*n*1 = O*n*2	1.66	0.123	
C*n*1-C*n*2	0.764	0.148	
Bond angle	${}^{K}\theta_n$ (kJ mol^{-1})	θ_n (degree)	
CG*n*-O*n*1-C*n*1	635	117	
O*n*1-C*n*1 = O*n*2	700	122	
O*n*1-C*n*1-C*n*2	545	113	
O*n*2 = C*n*1-C*n*2	750	125	
Improper dihedral	${}^{K}\xi_n$ (kJ mol^{-1} degree^{-2})	ξ_n (degree)	
C*n*1-C*n*2-O*n*1-O*n*2	0.051	0.0	
Dihedral angle	${}^{K}\phi_n$ (kJ mol^{-1})	cos(δ_n)	m_n
-CG*n*-O*n*1-	3.77	+1	3
-O*n*1-C*n*1-	16.7	−1	2
-C*n*1-C*n*2-	1.0	+1	6

heating phase. The corresponding decrease in density is about 13% relative to the start-up value. A_c is stable at 0.230 nm^2 (Table 4).

The starting coordinates for the simulation of model M3 are taken from the end of the heating phase of the M2 simulation, where the system has expanded considerably relative to the initial set-up. The system relaxes quickly and then undergoes an additional phase of equilibration (Fig. 3). The *x* dimension reduces to 4.8 nm with further minor reduction at 1.6 ns. Correspondingly, the *y* dimension, which drops at first, rises to 12.3 nm. The *z* dimension also undergoes a step-like adjustment to 4.9 nm at about the same time point. The volume is stable at 293 nm^3, the corresponding decrease in density from the estimated initial value being about 0.8%. The equilibrium value of A_c is 0.197 nm^2 (Table 4).

The coordinates from an equilibrated test run are taken to start the M4 simulation and so the starting box dimensions are close to those of the equilibrated system. The *x* dimension has a plateau value of 4.9 nm. In the *y* dimension the equilibrated value is 12.0 nm. The *z* dimension is stable at 4.9 nm. The average volume is 292 nm^3, implying a minute decrease in density, relative to the start-up value, of 0.3%. The value of A_c is very close to that of M3 at 0.197 nm^2 (Fig. 3, Table 4).

As in the case of models M3 and M4 discussed above, while models M5 and M6 have a similar average volume and area, the individual box dimensions do not coincide (Fig. 3, Table 4). In M5, the *x* dimension is 5.1 nm and the *y* dimension is 13.0 nm, whereas in M6 the *x* dimension is 5.2 nm and the *y* dimension is 12.7 nm. The average value in the *z* dimension stabilizes in M5 at 4.9 nm and in M6 at 4.8 nm. M5 has a mean volume of 320 nm^3, which corresponds to a decrease in density of 10%. In M6 the volume is 318 nm^3, the corresponding decrease in density being similar. The mean square area per chain, A_c, is approximately 0.220 nm^2 in both cases (Table 4).

In all six simulations the *z* dimension decreases relative to the initial value of 5.1 nm. In no case does A_c decrease below the initial value of 0.192 nm^2 (Fig. 3). For a summary of the average dimensions obtained from the equilibrated trajectories, see Table 4.

Chain flexibility and dynamics

To examine the overall mobility of the system in the different models, we evaluate the dynamics of the torsion angles along each chain. The number of transitions observed per dihedral angle is reported in Table 5. The definition of the transition follows the standard convention used in GROMOS96, where a transition is said to have occurred if the dihedral angle passes to the bottom of the adjacent well in the dihedral energy term (van Gunsteren et al. 1996). In each case, the transitions are counted over 2.5 ns of the equilibrated trajectory. Specifically, we report the average number of transitions per dihedral angle in 100 ps, with the number for each dihedral averaged over the entire triglyceride array. Also reported is the percentage of time that each dihedral angle remains in the *trans* conformation. This is evaluated by simply counting the number of times the dihedral angle is in the *trans* well (beyond |120°|). The results for each model are shown in Table 6.

The general pattern of behaviour of all six models is similar. We examine the dihedral angles individually. The torsion about the bond between the glycerol carbon CG*n* and the ester oxygen O*n*1 shows evidence of some transitions. No transition is seen about the planar ester bond during the entire course of the simulation. The torsion about the bond between the ester carbon, C*n*1, and the first methylene of the chain, C*n*2, being a rotation about a bond connecting an sp^2 and an sp^3 atom, undergoes more or less free rotation, with the *cis* conformation disallowed by steric repulsion. As the actual

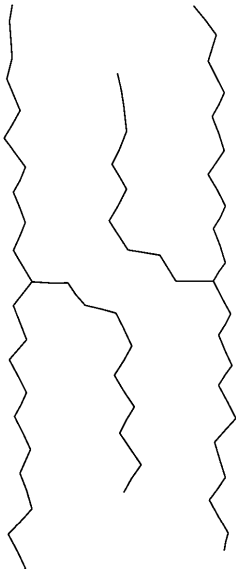

Fig. 2 Schematic representation of the double-layer packing mode seen in the gel or α phase of triglycerides

number of transitions in this case is irrelevant, they are not listed in Table 5.

Of particular interest are the torsional angles about the bonds connecting the sp^3 alkane carbons. The number and frequency of transitions increases as one proceeds towards the chain termini, although the actual number of transitions is small. The behaviour of the three chains is similar in each model, although in each model the degree and gradient of flexibility of chain 3 seems slightly greater (Table 5). This appears to have little effect on the percentage of *trans* conformations in the chain. There are a comparable number of *trans* conformations per dihedral angle as one proceeds down any of the chains in each model (Table 6). The dihedral -C13-C14- of model M1 undergoes a relatively large number of transitions. As we will see in the discussion section, this is a direct consequence of the relative rigidity and close-packed nature of the molecules in this model.

Molecular conformation and layer structure

A typical molecular conformation from each of the six simulations is shown in Fig. 4. In simulations M1 and M4, the chair conformation is preserved. In the case of

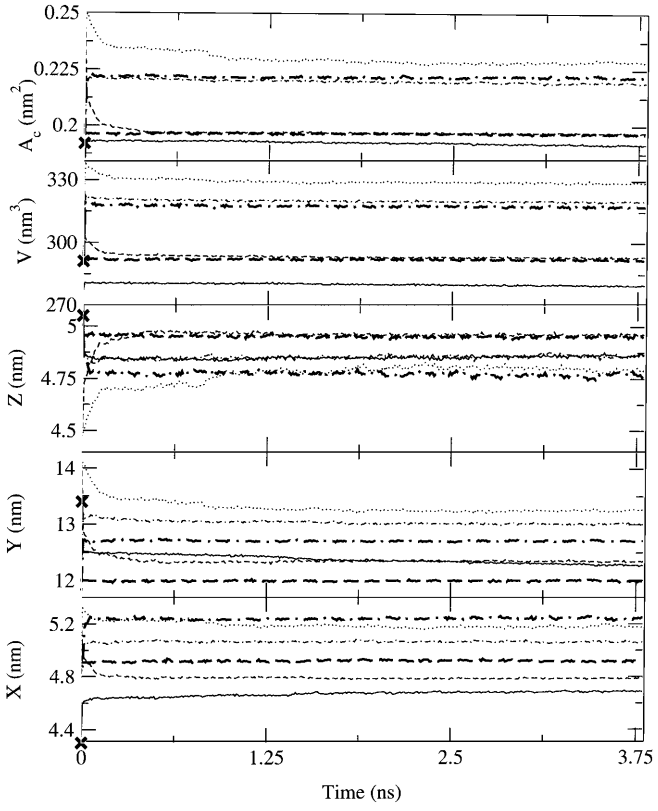

Fig. 3 Variation in the volume, V, and dimensions, x, y and z, of the periodic box and in the square area per chain, A_c, as a function of time: M1 (*solid line*), M2 (*dotted line*), M3 (*thin dashed line*), M4 (*thick dashed line*), M5 (*thin dot-dash line*), M6 (*thick dot-dash line*). The values from the initial set-up are marked in *crosses* on the ordinate. The plots begin after the initial heating phase of the simulations in the case of M1 and M2 and from intermediate structures in the case of the other simulations

M2, the structure changes to resemble the tuning-fork form. We refer here to the general form of the molecule, as opposed to the relative juxtaposition of the different chains that may also be referred to by the same term (van Langevelde et al. 2000). In simulations M3 to M6 the structure lies somewhere in between the two forms.

The planarity of the layers is evaluated by calculating the root-mean-square atom positional deviation (RMSD) in the z direction for the central glycerol carbon, CG2, of each molecule from its mean (over the 100 molecules in the layer) position, in each of the layers. The results, averaged over the equilibrated trajectories,

Table 4 Dimensions of the periodic computational box in the x, y and z directions averaged over 2.5 ns of equilibrated trajectory for each of the models M1 to M6. The volume of the periodic box is indicated by V and the mean square area per alkane chain, perpendicular to the chain direction, by A_c. The respective values for the initial system are also given

	Initial estimate	M1	M2	M3	M4	M5	M6
x (nm)	4.30	4.70	5.18	4.79	4.91	5.07	5.24
y (nm)	13.40	12.30	13.25	12.30	12.00	13.03	12.71
z (nm)	5.05	4.80	4.80	4.96	4.95	4.85	4.77
V (nm^3)	291	280	329	293	292	320	318
A_c (nm^2)	0.192	0.192	0.230	0.197	0.197	0.220	0.221

Table 5 The number of transitions per torsion angle per 100 ps, averaged over 2.5 ns of equilibrated trajectory in each of the simulation models M1 to M6. The transitions are taken as defined in van Gunsteren et al. (1996), i.e. the transitions are taken to be completed when the torsion angle assumes the value at the bottom of the adjacent torsion angle well, rather than if it merely crosses the top of the torsional barrier

Torsion angle	M1	M2	M3	M4	M5	M6
Chain 1						
-CG1-O11-	0.2	0.1	0.6	0.5	0.2	0.1
-O11-C11-	_[a]	_[a]	_[a]	_[a]	_[a]	_[a]
-C11-C12-	_[b]	_[b]	_[b]	_[b]	_[b]	_[b]
-C12-C13-	0.1	1.7	0.4	2.0	2.0	2.1
-C13-C14-[c]	21.2	9.8	1.9	0.6	7.0	2.5
-C14-C15-	0.5	2.7	0.3	1.0	2.1	4.2
-C15-C16-	6.2	19.5	2.6	1.9	17.4	15.0
-C16-C17-	9.5	16.6	6.2	6.4	15.2	18.3
Chain 2						
-CG1-CG2-	0.0	0.2	0.1	0.3	0.3	0.01
-CG2-O21-	0.0	0.1	0.3	2.1	0.8	1.1
-O21-C21-	_[a]	_[a]	_[a]	_[a]	_[a]	_[a]
-C21-C22-	_[b]	_[b]	_[b]	_[b]	_[b]	_[b]
-C22-C23-	0.8	12.6	1.3	0.7	2.9	2.3
-C23-C24-	0.2	1.5	0.3	2.0	1.8	1.6
-C24-C25-	1.7	9.0	0.6	0.4	3.2	3.8
-C25-C26-	0.6	9.8	1.6	4.3	9.4	11.2
-C26-C27-	2.5	21.6	6.0	5.0	13.8	17.2
Chain 3						
-CG2-CG3-	0.3	0.1	0.1	0.0	0.01	0.0
-CG3-O31-	0.1	0.03	1.7	0.6	0.01	0.0
-O31-C31-	_[a]	_[a]	_[a]	_[a]	_[a]	_[a]
-C31-C32-	_[b]	_[b]	_[b]	_[b]	_[b]	_[b]
-C32-C33-	0.3	1.4	0.1	0.04	0.2	0.3
-C33-C34-	0.1	7.5	1.3	3.3	5.1	8.2
-C34-C35-	1.0	5.2	1.0	0.8	3.5	4.2
-C35-C36-	2.1	15.1	3.6	6.0	12.2	16.2
-C36-C37-	14.1	30.4	23.7	21.3	31.0	30.1

[a]This is the torsion about the planar ester bond and undergoes no transitions during the course of the simulations

[b]This torsion angle has a low barrier to rotation (1 kJ mol^{-1}; see Table 3) and shows almost free rotation

[c]The significantly larger number of transitions seen in model M1 are discussed in the text and arise as a consequence of the close-packed nature of the molecules during simulation

are shown in Table 7. In all simulations except M1 the layers reorganize within the periodic box during the simulation. This becomes evident when the RMSD values are of the order of half the z dimension. For the layers that reorganize, we subtract half the z-length from the calculated average. The mean RMSD is about 0.03 nm for each of the layers in M1, indicating that the system remains close to planar (Table 7). The RMSD of CG2 in model M2 is an order of magnitude greater than in M1. In models M3 and M4 the spread in z is fairly small, indicating that the layers retain their identity. The models M5 and M6 have a larger spread in the position of CG2.

We measure the collective tilt of the molecules with respect to the layer normal in each layer. To do so we choose a relevant molecular vector whose orientation we assess with respect to the z-axis, which is collinear with the layer normal. As discussed above, there is little mobility in the chains, which remain more or less all-*trans* (Tables 5 and 6). Therefore, we find that the terminal carbons C18, C28 or C38 serve as well as the internal carbons of the chain such as C16, C26 or C36 to determine the end-points of the vector defined below, whose tilt is measured. For the system where the molecules retain the chair conformation (M1), we evaluate the tilt of the vector C38-C18 that runs along the collinear chains 3 and 1. For the remaining systems, where the tuning-fork conformation dominates, we use the sum of the tilt of the two opposing vectors C38-C18 and C38-C28. The average tilt in each layer for each of the models is shown in Table 7. There is a systematic tilt of approximately 15° in each layer for model M1. In model M2, where the tuning-fork conformation is seen, the average tilt per layer is small, about 1°. Models M3 to M6 show similar low values.

Lastly, the interdigitation of the chains in the plane of the double layer is evaluated. In the chair conformation the adjacent chains 1 and 2 of the triglyceride molecule are staggered in the z dimension. When two double layers are juxtaposed, the longer chains (chains 1 or 3) of one layer slot into the space made available by the shorter chains (chain 2). This results in an inter-locking or interdigitation of the chains at the double-layer interphase. The difference in the z dimension of the terminal carbons C18 and C28 for each of the four layers, averaged over the 100 molecules in the layer, is calculated. The average

Table 6 The percentage of time that each torsion angle remains in the *trans* conformation, as evaluated from 2.5 ns of equilibrated trajectory for each of the simulation models, M1 to M6. The residence time is evaluated by counting the time that the torsion angle remains in the *trans* well, i.e. beyond |120°|. The results are averaged over the molecular array and over the number of time steps. The percentages of *trans* conformations, averaged per alkane torsion angle and over the total number of torsion angles in the molecule, are shown in the last two rows

Torsion angle	M1	M2	M3	M4	M5	M6
Chain 1						
-CG1-O11-	98	98	95	95	97	99
-O11-C11-[a]	100	100	100	100	100	100
-C11-C12-	_[b]	_[b]	_[b]	_[b]	_[b]	_[b]
-C12-C13-	99	82	98	88	88	88
-C13-C14-	71	74	94	94	76	85
-C14-C15-	93	76	95	90	79	82
-C15-C16-	75	77	80	85	78	74
-C16-C17-	74	79	76	74	77	77
Chain 2						
-CG1-CG2-	100	97	99	96	96	99
-CG2-O21-	100	99	98	82	95	91
-O21-C21-[a]	100	100	100	100	100	100
-C21-C22-	_[b]	_[b]	_[b]	_[b]	_[b]	_[b]
-C22-C23-	86	72	86	95	81	87
-C23-C24-	97	85	96	90	83	87
-C24-C25-	86	76	91	95	78	78
-C25-C26-	92	77	84	77	74	74
-C26-C27-	80	83	74	75	78	79
Chain 3						
-CG2-CG3-	99	95	99	100	99	100
-CG3-O31-	98	99	92	95	99	100
-O31-C31-[a]	100	100	100	100	100	100
-C31-C32-	_[b]	_[b]	_[b]	_[b]	_[b]	_[b]
-C32-C33-	96	91	99	99	96	96
-C33-C34-	97	75	85	85	72	76
-C34-C35-	85	74	89	90	71	79
-C35-C36-	80	79	75	76	76	78
-C36-C37-	78	79	78	80	79	78
% *trans*: alkane torsions	86	79	87	86	79	81
% *trans*: all torsions	91	86	91	90	86	87

[a]This is the torsion angle about the planar ester bond and undergoes no transitions during the course of the simulations

[b]This torsion angle has a low barrier to rotation (1 kJ mol^{-1}; see Table 3) and shows almost free rotation

value for each layer in each of the four models is shown in Table 7. In M1, the z displacement is approximately 0.2 nm in each layer, suggesting that the staggering of the chains is possible from spatial considerations. In M2 to M6 this value is close to 0, indicating that the chain termini are practically coplanar.

Figure 5 shows snapshots of the system, which illustrate the ordering of the layers in the six models.

Discussion

All the models remain in the gel phase, as evaluated by the average cross-sectional area per chain, A_c. This is a more appropriate parameter to use in the assessment of phase behaviour than properties such as the volume or density. Indeed, the area per lipid is frequently taken as the order parameter of phase transition (Israelachvilli 1995). It should be noted that the measured values of the area per chain for hydrated DPPC gels, which unlike triglycerides in the gel phase are tilted, lie between 0.22 and 0.24 nm^2 (Tardieu et al. 1973; Wiener et al. 1989; Tristram-Nagle et al. 1993). Assuming a tilt angle of approximately 30°, the area per chain in the plane perpendicular to the chain, equivalent to what we refer to as A_c, is believed to lie between 0.19 and 0.20 nm^2 for DPPC (Tristram-Nagle et al. 1993; Nagle and Tristram-Nagle 2000; Petrache et al. 2000). It is equal to 0.21 nm^2 for the untilted dilauroylphospatidylethanolamine (McIntosh and Simon 1986). From the dimensions of hexagonal sub-cells of long-chain compounds (Abrahamsson et al. 1978), one could conclude that, at the outer limit, A_c is equal to 0.23 nm^2. In effect, an acceptable range of gel phase values for A_c is 0.19–0.23 nm^2. As seen in Table 4, A_c is close to the start-up value of 0.192 nm^2 in model M1. Models M2 to M6 expand, as was anticipated for all the models when the system was set up. The expansion is relatively large in the case of M2 (A_c is 0.23 nm^2), although the system may still be accepted as being in the gel phase. The structure and organization of the liquid phase of triglycerides is not fully characterized (Larsson 1986;

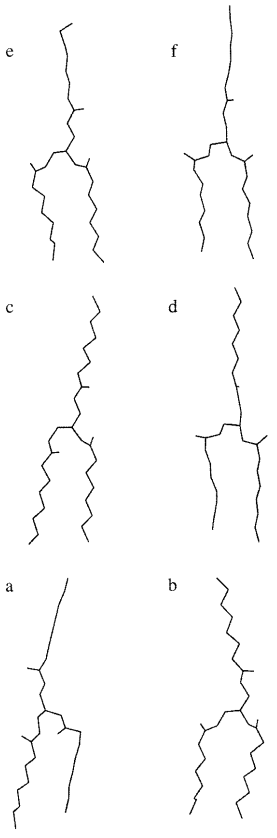

Fig. 4 Typical molecular conformations for each of the models at the end of 2.5 ns of simulation: **a** M1, **b** M2, **c** M3, **d** M4, **e** M5, **f** M6

Hernqvist 1988; Povey 1994). Models M3 and M4, that were simulated with identical aliphatic alkane parameter sets and differ only in the partial charges at the glycerol ester group, have the same A_c of 0.20 nm^2. Similarly, models M5 and M6 have identical values of A_c of 0.22 nm^2.

In all of the models we see a reduction in the z dimension relative to the initial value. The initial value of z was set equal to the length of the molecule in the extended all-*trans* state. Does the reduction in z take place due to torsional relaxation? The number of transitions per dihedral angle is small, generally less than 20 per 100 ps, with the exception of the terminal dihedral angles of the third chain (Table 5). In all the models we see an increase in the number and frequency of transitions towards the chain termini (Table 5). This is supported by experimental evidence. The first moments from ^{2}H NMR spectra of DPPC in the gel phase imply a gradient in the flexibility of the chains, even in the gel phase (Davis 1983). All the dihedral angles remain in the *trans* conformation for over 70% of the time (Table 6). Experimental evidence suggests that the number of *trans* bonds in the gel phase is between 93% and 98% (Davis 1983). In all the simulations reported here the number of *trans* bonds is on the low side. When averaged over all the dihedral angles listed in Table 6, the percentage of *trans* bonds is about 90% in models M1, M3 and M4 and about 86% in models M2, M5 and M6. The number is slightly lower when the alkane dihedral angles alone are taken into consideration. Kink formation in the alkyl chain is frequently invoked to explain mobility in the spatially restricted gel phase (Träuble and Haynes 1971). There is some evidence of kink formation, as seen in the snapshots of the simulations (Fig. 5). In general, the torsional behaviour of all six models is consistent with the gel phase. However, the low chain mobility in some cases suggests that the reduction in z cannot be fully explained as due to a melting of the chain termini.

We consider each model individually. In model M1 the molecule remains in the chair form (Fig. 4a). There is little flexibility in the chains; indeed, with the exception of dihedral angle -C13-C14-, this model undergoes the smallest number of transitions (Table 5). The proportion of *trans* conformations, evaluated over the equilibrated trajectories, is 91% (Table 6). There is evidence of kink formation (Fig. 5a) and, despite the transitions that do occur, chain packing is not significantly perturbed. As noted earlier, there is little increase in A_c compared to the relatively low initial value of 0.19 nm^2 (Table 4). The individual layers remain essentially planar, as seen by the small spread in the position of atom CG2 (Table 7). The chains are interdigitated, locking the layer interface (Fig. 5a). An interesting effect of the close-packing and inter-locking of the chains is the following. Chain 1 and chain 2 are adjacent and essentially all-*trans*. When chain 2, which is shorter, terminates, the next methylene carbon of chain 1, namely C15 (see Fig. 1 for clarification of nomenclature), is able to fluctuate in the available space. This explains the increased mobility of the corresponding -C13-C14- torsional angle (Table 5). Mobility of the following carbon C16 (torsion -C14-C15-) is more restricted due to the observed chain interdigitation. The longer chain from the juxtaposed double layer protrudes into the pocket.

The rigidity in M1 is compensated for by a collective tilting of the chains (Fig. 5a). The measured tilt in M1 is 16° (Table 7), a number that nicely rationalizes the 'observed reduction in z [$z_{initial} \times \cos(16) = 4.8$ nm, where $z_{initial} = 5$ nm]. Chain tilting is observed in single crystals of amphipathic lipids (for example, Hauser et al. 1981) as well as in triglycerides in the β forms (Jensen and Mabis 1966; de Jong 1980; van Langevelde et al. 2000; Sato et al. 2001). Tilting of the molecule is also seen in the gel $L_{\beta'}$ phases of polar lipids such as DPPC (Tristram-Nagle et al. 1993). However, it is known that triglycerides in the gel phase are not tilted. The melting behaviour of triglyceride gels does not show the chain-length dependent alternation characteristic of tilted systems where odd-even chain-length effects are seen (Hagemann 1988). The chain tilt in model M1 is clearly an artefact of the parameter set, an effect that has been observed in the past (Bareman and Klein 1990; Chandrasekhar 1992). The measured tilt confirms that

Table 7 Structural features of the different models

	RMSD from mean z position of the central glycerol carbon CG2 (nm)	[a]Mean systematic tilt of the vector defined by C38-C18 (model M1) and the sum of the tilts of the vectors C38-C18 and C38-C28 (models M2-M6) w.r.t. the z axis (°)	Mean separation in the z direction between terminal chain atoms C18 and C28 (nm)
M1			
Layer 1	0.03	15.1	0.19
Layer 2	0.03	15.0	–0.19
Layer 3	0.03	16.8	0.19
Layer 4	0.03	16.1	–0.19
M2			
Layer 1	0.20	0.6	0.04
Layer 2	0.40	1.1	–0.01
Layer 3	0.30	–1.2	0.02
Layer 4	0.30	1.5	–0.01
M3			
Layer 1	0.10	2.2	0.05
Layer 2	0.02	–1.5	–0.05
Layer 3	0.10	–3.2	0.08
Layer 4	0.10	2.7	–0.08
M4			
Layer 1	0.20	–0.7	0.00
Layer 2	0.20	1.2	0.04
Layer 3	0.10	–1.3	0.00
Layer 4	0.10	–1.6	0.03
M5			
Layer 1	0.50	0.3	0.02
Layer 2	0.10	0.0	0.02
Layer 3	0.20	–0.7	0.02
Layer 4	0.20	1.3	0.01
M6			
Layer 1	0.50	0.2	0.01
Layer 2	0.50	0.8	0.02
Layer 3	0.05	–4.0	0.00
Layer 4	0.05	–0.7	0.01

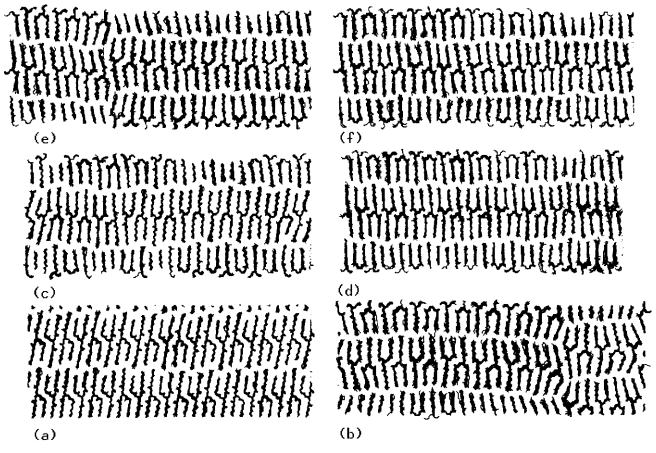

Fig. 5 Snapshot of each of the model systems at the end of 2.5 ns of simulation: **a** M1, **b** M2, **c** M3, **d** M4, **e** M5, **f** M6. The orthographic projection is of the y-z plane of the computational box. The molecular array in both x and y directions contains 10 molecules

model M1 based on the parameter set 43A2 has serious defects for lipid simulations.

In model M2 the molecule goes to a tuning-fork conformation during equilibration (Fig. 4b). The conformational change reduces the length of the molecule by at least one methylene. There is greater chain mobility, particularly at the termini (Table 5), which is a consequence of the larger square area ($A_c = 0.23$ nm^2) available per chain (Table 4). The number of *trans* conformations is only 86% (Table 6). These effects contribute to a decrease in the z dimension from the extended all-*trans* length and also result in a lack of chain interdigitation. There is a large spread in the z position of the glycerol carbon (Table 7). This is due to the fact that the layers are fragmented, the different fragments being shifted or staggered in the z direction (Fig. 5b). Clearly, the use of a shallow potential energy term with a large radius (type CH_0) to characterize the ester carbon perturbs both the molecular conformation and the lamellar organization.

In the case of model M3 we see a favourable expansion in A_c. Indeed, the average value of 0.197 nm^2 is close to the value of 0.199 nm^2 calculated for the gel phase from fully hydrated DPPC (Wiener et al. 1989). Here the molecules are chair-like (Fig. 4c), although the termini of chains 1 and 2 are no longer staggered (Fig. 4c, Table 7), obscuring chain interdigitation at the layer interface (Fig. 5c). The expansion in the plane of the bilayer relative to the initial set-up (Table 4) results

in a greater number of transitions at the glycerol backbone than in the alkane chain (compare, for example, the transition in dihedral angle -CG*n*-O*n*1- in models M1, M2 and M3 in Table 5), although the numbers remain small. The total number of *trans* conformations is 91%, which compares well with experiment (Davis 1983). It seems that the reduction in the z dimension is entirely due to torsional reorientation. There is no significant collective molecular tilt (Table 7), but one observes a rippling of the layers (Fig. 5c) that could either be a natural characteristic of the system (Nagle and Tristram-Nagle 2000; Marrink and Mark 2001) or arise as result of the type of cut-off used (Tobias et al. 1997). The rippling causes little perturbation in the planarity of the system (Table 7). In general the system behaves in the classical manner for the gel phase. The parameter set 45A3 used in model M3 may be regarded as satisfactory.

Model M4 makes use of the same aliphatic alkane parameters as model M3 (Table 1), but has a different set of partial charges at the glycerol ester group (Table 2). The behaviour of this model is similar to that of model M3 (Tables 5, 6, 7, Figs. 4 and 5). The ab initio charges of Chiu et al. (1995), when combined with the 45A3 parameters in simulations of fully hydrated DPPC, result in an expansion in the mean square area per molecule (Schuler 2000). However, when adapted for the neutral triglycerides with less polarity and no hydration, the change in partial charges has little effect. Indeed, the only notable difference is that despite the similar area attained by the two models, the expansion in the x and y directions is different. The larger charges due to Chiu et al. (1995) used in model M4 result in a greater repulsion along the shorter x dimension and a greater attraction in the longer y dimension than in model M3 (Fig. 3, Table 4).

As in the two cases above, models M5 and M6, which differ only in the partial charges used at the glycerol ester group (Table 2), show an overall similarity of structural (Table 7, Fig. 4e and f, Fig. 5e and f) and dynamic (Tables 5 and 6) behaviour. The molecular structures resemble a tuning fork (Fig. 4e and f) and show no evidence of interdigitation (Table 7). There is no collective molecular tilt (Table 7, Fig. 5e and f). In model M5 there is evidence of layer fragmentation not seen in model M6 (Fig. 5e and f). The increased size of the planar ester carbon used in these simulations (0.5773 nm; see Table 1) when compared with that used in models M3 and M4 (0.3361 nm) has an effect on the dimensions and mobility of the system. In both models M5 and M6 the value of A_c is the same and is equal to 0.22 nm^2, although here too the expansion in the x and y directions is different (Fig. 3, Table 4). As in model M2, the larger value of A_c in models M5 and M6 results in a greater number of dihedral angle transitions along the chain (Table 5). The number of *trans* conformations of 86% is underestimated relative to the experimental value of 92–98% (Davis 1983).

To summarize, the refined parameter set 45A3 for the united atom aliphatic alkane carbons significantly improves the performance of the simulations of the triglyceride trioctanoin in the gel phase. Variation in the parameters of the ester carbon has a marked effect on the simulations. For example, the large radius of the ester carbon in set 45A3-45 results in too large an area per chain. In contrast, the use of higher charges for the ester group does not greatly affect the simulations. This is evident when comparing models M3 and M4 that use parameter set 45A3 or models M5 and M6 that are run with the parameter set 45A3-45×12. In conclusion, the parameter set 45A3, where the refined alkane parameters are combined with an ester carbon of radius 0.34 nm, performs well in comparison to the other parameter sets and successfully reproduces the structural and dynamic features of the model.

Acknowledgements We would like to thank Christine Peter, Lukas Schuler and Xavier Daura for discussions and advice.

References

Abrahamsson S, Dahlén B, Löfgren H, Pascher I (1978) Lateral packing of hydrocarbon chains. Prog Chem Fats Other Lipids 16:125–143

Bailey AE, Singleton WS (1945) Dilatometric investigations of fats III. The density, expansibility, and melting dilation of some simple triglycerides and other fats. Oil Soap 22:265–271

Bareman G, Klein M (1990) Collective tilt behaviour in dense, substrate-supported monolayers of long-chain molecules: a molecular dynamics study. J Chem Phys 93:7483–7491

Berendsen HJC, Postma JPM, Gunsteren WF van, DiNola A, Haak JR (1984) Molecular dynamics with coupling to an external bath. J Chem Phys 81:3684–3690

Birker JMWL, Jong S de, Roijers EC, Soest T van (1991) Structural investigations of β' triacylglycerols: an X-ray diffracton and microscopic study of twinned β' crystals. J Am Oil Chem Soc 68:895–906

Bogusz S, Venable RM, Pastor RW (2000) Molecular dynamics simulations of octyl glucoside micelles: stuctural properties. J Phys Chem B 104:5462–5470

Callaghan PT, Jolley KW (1977) An irreversible liquid-liquid phase transition in tristearin. J Chem Phys 67:4773–4774

Cevc G, Marsh D (1987) The physical chemistry of lipids. Wiley-Interscience, New York

Chandrasekhar I (1986) A constraint algorithm for molecular dynamics simulation and an analysis of lipid conformation. PhD thesis, Indian Institute of Science, Bangalore, India

Chandrasekhar I (1992) Parameter development for molecular dynamics simulation of lipids. In: Gaber BP, Easwaran KRK (eds) Biomembrane structure and function – state of the art. Adenine Press, Albany, NY, pp 353–363

Chandrasekhar I, Sasisekharan V (1989) The nomenclature and conformational analysis of lipids and lipid analogues. Mol Cell Biochem 91:173–182

Chapman D, Richards RE, Yorke RW (1960) Nuclear resonance spectra of the polymorphic forms of glycerides. J Chem Soc 436–444

Chiu SW, Clark M, Subramaniam S, Scott HL, Jakobsson E (1995) Incorporation of surface tension into molecular dynamics simulation of an interface: a fluid phase lipid bilayer membrane. Biophys J 69:1230–1245

Chiu SW, Clark M, Jakobsson E, Subramaniam S, Scott HL (1999) Optimisation of hydrocarbon chain interaction parameters:

application to the simulation of fluid phase bilayers. J Phys Chem B 103:6323–6327
Daura X, Mark AE, Gunsteren WF van (1998) Parametrization of aliphatic CHn united atoms of GROMOS96 force field. J Comput Chem 19:535–547
Davis JH (1983) The description of membrane lipid conformation, order and dynamics by ^{2}H-NMR. Biochim Biophys Acta 737:117–171
Egberts E, Berendsen HJC (1988) Molecular dynamics simulation of a smectic liquid crystal with atomic detail. J Chem Phys 89:3718–3732
Egberts E, Marrink S-J, Berendsen HJC (1994) Molecular dynamics simulation of a phospholipid membrane. Eur Biophys J 22:423–436
Feller SE, Yin D, Pastor RW, MacKerell D Jr (1997) Molecular dynamics simulation of unsaturated lipid bilayers at low hydration: parametrization and comparison with diffraction studies. Biophys J 73:2269–2279
Garti N, Sato K (eds) (1988) Crystallisation and polymorphism of fats and fatty acids. Dekker, New York
Goto M, Kodali DR, Small DM, Honda K, Kozawa K, Uchida T (1992) Single crystal structure of a mixed-chain triacylglycerol: 1,2-dipalmitoyl-3-acetyl-*sn*-glycerol. Proc Natl Acad Sci USA 89:8083–8086
Gunsteren WF van, Berendsen HJC (1990) Computer simulation of molecular dynamics: methodology, applications and perspectives in chemistry. Angew Chem Int Ed Engl 29:992–1023
Gunsteren WF van, Billeter SR, Eising AA, Hünenberger PH, Krüger P, Mark AE, Scott WRP, Tironi IG (1996) Biomolecular simulation: the GROMOS96 manual and user guide. Hochschulverlag ETH-Zürich/Biomos, Zürich/Groningen
Hagemann J (1988) Thermal behaviour and polymorphism of acylglycerides. In: Garti N, Sato K (eds) Crystallisation and polymorphism of fats and fatty acids. Dekker, New York, pp 9–95
Hauser H, Pascher I, Pearson RH, Sundell S (1981) Preferred conformation and molecular packing of phosphatidylethanolamine and phosphatidylcholine. Biochim Biophys Acta 650:21–51
Heintz W (1849) Fette säuren in bassia-oel, shea-butter und chinesischem pflanzentalg. In: Liebig J, Kopp H (eds) Jahresbericht über die Fortschritte der reinen, pharmaceutischen und technischen Chemie, Physik, Mineralogie und Geologie 2. Ricker'sche Buchhandlung, Giessen, Germany, pp 342–344
Hernqvist L (1988) Crystal structures of fats and fatty acids. In: Garti N, Sato K (eds) Crystallisation and polymorphism of fats and fatty acids. Dekker, New York, pp 97–137
Husslein T, Newns DM, Pattnaik PC, Zhong Q, Moore PB, Klein ML (1998) Constant pressure and temperature molecular-dynamics simulation of the hydrated diphytanolphosphatidylcholine lipid bilayer. J Chem Phys 109:2826–2832
Israelachvilli JN (1995) Intermolecular and surface forces. Academic Press, New York
Jensen LH, Mabis AJ (1966) Refinement of the structure of β-tricarpin. Acta Crystallogr 21:770–781
Jong S de (1980) The triacylglycerol crystal structures and fatty acid conformation. PhD thesis, University of Utrecht, The Netherlands
Jong S de, Soest TC van, Schaik MA van (1991) Crystal structures and melting points of unsaturated triacylglycerols in the β phase. J Am Oil Chem Soc 68:371–377
Kishore K, Shobha HK (1992) Thermodynamics of flow and vaporization processes in long-chain liquids. J Phys Chem 96:8161–8168
Langevelde A van, Malssen K van, Driessen R, Goubitz K, Hollander F, Peschar R, Zwart P, Schenk H (2000) Structure of $C_nC_{n+2}C_n$-type (n = even) β' triacylglycerols. Acta Crystallogr Sect B 56:1103–1111
Larsson K (1963) The crystal structure of the 1,3-diglyceride of thiadodecanoic acid. Acta Crystallogr 16:741–747
Larsson K (1986) Physical properties – structural and physical characteristics. In: Gunstone FD, Harwood JL, Paley FB (eds) The lipid handbook. Chapman and Hall, London, pp 335–377
Lutton ES (1950) Review of the polymorphism of saturated even glycerides. J Am Oil Chem Soc 27:276–283
Malkin T (1954) The polymorphism of glycerides. Prog Chem Fats Other Lipids 2:1–50
Marrink S-J, Mark AE (2001) Effect of undulations on surface tension in simulated bilayers. J Phys Chem B (in press)
McGowan JC (1982) Isothermal compressibility of liquids. In: Weast RC, Astle MJ (eds) CRC handbook of chemistry and physics. CRC Press, Boca Raton, pp F14–F18
McIntosh TJ, Simon SA (1986) Area per molecule and distribution of water in fully hydrated dilauroylphosphatidylethanolamine bilayers. Biochemistry 25:4948–4952
Merz K, Roux B (eds) (1996) Biological membranes: a molecular perspective from computation and experiment. Birkhauser, Boston
Nagle JF (1993) Evidence for partial rotational order in gel phase DPPC. Biophys J 64:1110–1112
Nagle JF, Tristram-Nagle S (2000) Structure of lipid bilayers. Biochim Biophys Acta 1469:159–195
Pastor RW (1994) Molecular dynamics and Monte Carlo simulations of lipid bilayers. Curr Opin Struct Biol 4:486–492
Petrache HI, Dodd SW, Brown MF (2000) Area per lipid and acyl chain length distributions in fluid phosphatidylcholines determined by ^{2}H NMR spectroscopy. Biophys J 79:3172–3192
Povey MJW (1994) Analysis of lipid structure by neutron diffraction. In: Tyman JHP, Gordon MH (eds) Developments in the analysis of lipids. Royal Society of Chemistry, Cambridge, pp 161–178
Ramachandran GN, Sasisekharan V (1969) Conformation of polypeptides and proteins. Adv Protein Chem 23:283–437
Ryckaert JP, Ciccotti G, Berendsen HJC (1977) Numerical integration of the cartesian equations of motion of a system with constraints: molecular dynamics of n-alkanes. J Comput Phys 23:327–341
Sato K, Goto M, Yano J, Honda K, Kodali DR, Small DM (2001) Atomic resolution structure analysis of β' polymorph crystal of a triacylglycerol: 1,2-dipalmitoyl-3-myristoyl-*sn*-glycerol. J Lipid Res 42:338–345
Schlenkrich M, Brickmann J, MacKerell AD Jr, Karplus M (1996) An empirical potential energy function for phospholipids: criteria for parameter optimization and applications. In: Merz K, Roux B (eds) Biological membranes: a molecular perspective from computation and experiment. Birkhauser, Boston, pp 31–81
Schuler LD (2000) Molecular dynamics simulation of aggregates of lipids: development of force-field parameters and application to membranes and micelles. PhD thesis, ETH-Zürich, Switzerland
Schuler LD, Gunsteren WF van (2000) On the choice of dihedral angle potential energy functions for n-alkanes. Mol Simulation 25:301–319
Schuler LD, Daura X, Gunsteren WF van (2001) An improved GROMOS96 force field for aliphatic hydrocarbons in the condensed phase. J Comput Chem 22:1205–1218
Small DM (1986) In: Hanahan D (ed) The physical chemistry of lipids from alkanes to phospholipids. (Handbook of lipid research series 4) Plenum, New York, pp 1–672
Smondyrev AM, Berkowitz ML (2000) Molecular dynamics of the structure of dimyristoylphosphatidylcholine bilayers with cholesterol, ergosterol and lanosterol. Biophys J 80:1649–1658
Soest TC van, Jong S de, Roijers EC (1990) Crystal structures and melting points of saturated triacylglycerols in the β-3 phase. J Am Oil Chem Soc 67:415–423
Stouch TR, Ward KB, Altieri A, Hagler AT (1991) Simulation of lipid crystals: characterisation of potential energy functions and parameters for lecithin molecules. J Comput Chem 12:1033–1046
Tardieu A, Luzzati V, Reman FC (1973) Structure and polymorphism of the hydrocarbon chains of lipids: a study of lecithin-water phases. J Mol Biol 75:711–733
Tieleman DP, Berendsen HJC (1996) Molecular dynamics of a fully hydrated dipalmitoylphosphatidylcholine bilayer with different macroscopic boundary conditions and parameters. J Chem Phys 105:4871–4880

Tieleman DP, Marrink S-J, Berendsen HJC (1997) A computer perspective of membranes: molecular dynamics studies of lipid bilayer systems. Biochim Biophys Acta 1331:235–270

Tobias DJ, Tu K, Klein ML (1997) Atomic scale molecular dynamics simulations of lipid membranes. Curr Opin Colloid Interface Sci 2:115–126

Träuble H, Haynes DH (1971) The volume change in lipid bilayer lamellae at the crystalline-liquid crystalline phase transition. Chem Phys Lipids 7:324–335

Tristram-Nagle S, Zhang R, Suter RM, Worthington CR, Sun W-J, Nagle JF (1993) Measurement of chain tilt angle in fully hydrated bilayers of gel phase lecithins. Biophys J 64:1110–1112

Wiener MC, Suter RM, Nagle JF (1989) Structure of the fully hydrated gel phase of dipalmitoylphosphatidylcholine. Biophys J 55:315–325